Optimal finite-time heat engines under constrained control

Zhuolin Ye [1,*] Federico Cerisola [2,3] Paolo Abiuso [4,5] Janet Anders [3,6] Martí Perarnau-Llobet [5] and Viktor Holubec [7,†]

[1] *Institut für Theoretische Physik, Universität Leipzig, Postfach 100 920, D-04009 Leipzig, Germany*
[2] *Department of Materials, University of Oxford, Parks Road, Oxford OX1 3PH, United Kingdom*
[3] *Department of Physics and Astronomy, University of Exeter, Stocker Road, Exeter EX4 4QL, United Kingdom*
[4] *ICFO-Institut de Ciències Fotòniques, The Barcelona Institute of Science and Technology, 08860 Castelldefels (Barcelona), Spain*
[5] *Department of Applied Physics, University of Geneva, 1211 Geneva, Switzerland*
[6] *Institut für Physik und Astronomie, University of Potsdam, 14476 Potsdam, Germany*
[7] *Department of Macromolecular Physics, Faculty of Mathematics and Physics, Charles University, V Holešovičkách 2, CZ-180 00 Praha, Czech Republic*

(Received 25 February 2022; accepted 24 October 2022; published 22 November 2022)

We optimize finite-time stochastic heat engines with a periodically scaled Hamiltonian under experimentally motivated constraints on the bath temperature T and the scaling parameter λ. We present a general geometric proof that maximum-efficiency protocols for T and λ are piecewise constant, alternating between the maximum and minimum allowed values. When λ is restricted to a small range and the system is close to equilibrium at the ends of the isotherms, a similar argument shows that this protocol also maximizes output power. These results are valid for arbitrary dynamics. We illustrate them for an overdamped Brownian heat engine, which can experimentally be realized using optical tweezers with stiffness λ.

DOI: 10.1103/PhysRevResearch.4.043130

I. INTRODUCTION

The unprecedented improvement in experimental control over microscopic Brownian [1] and quantum systems [2–4] has induced a revolution in the study of heat engines [5,6]. It aims to generalize equilibrium and finite-time thermodynamics [7–15] to the nanoscale, where thermal and quantum fluctuations render thermodynamic variables such as work and heat stochastic [16]. Intense effort is devoted to uncover optimal performance of stochastic heat engines [16–41]. However, optimal control protocols are only known under approximations of fast [34–36] or slow [28,37–41] driving, or for specific microscopic models: engines based on overdamped Brownian particles in harmonic [24] or log-harmonic [42] potential, and underdamped harmonic Brownian heat engines [43]. Furthermore, most of these exact results are obtained under constraints on the state of the working medium [44], instead of experimentally motivated constraints on the control parameters [45,46]. An exception is Ref. [47], showing that reaching maximum efficiency of slowly driven cyclic heat engines requires control over the scaling of the full Hamiltonian to avoid heat leakages.

In this paper, we optimize finite-time thermodynamic cycles under constraints on control parameters such as trap stiffness of optical tweezers λ and bath temperature T. We show that, different from constraining the response such as the width σ of the phase distribution, constraining the control allows for surprisingly simple and general derivation of maximum-efficiency and maximum-power protocols. Besides other stark differences, for constrained control of Brownian heat engines, these protocols significantly outperform the protocol optimized for power and efficiency under constraints on σ [24].

The paper is organized as follows. In Sec. II, we introduce the considered setup with a periodically scaled Hamiltonian under experimentally motivated constraints. In Sec. III, we derive the corresponding maximum-efficiency protocol. In Sec. IV, we prove that the maximum-efficiency protocol yields, under certain conditions, also maximum output power. In Sec. V, we present a case study of optimization of power and efficiency for constrained control by considering a specific overdamped Brownian heat engine. Besides illustrating the general results derived in Secs. III and IV, we provide numerical evidence that the maximum-power protocol is, in this case, piecewise linear. We conclude in Sec. VI.

II. SETUP

Following Ref. [47], we assume that the Hamiltonian of the system that serves as a working medium of the stochastic heat engine is of the form

$$H(x,t) = \lambda(t) f(x), \tag{1}$$

*zhuolinye@foxmail.com
†viktor.holubec@mff.cuni.cz

where the control parameter $\lambda(t)$ periodically expands and shrinks the energy spectrum in time, and $f(x)$ is an arbitrary function of the system degrees of freedom x such that the equilibrium partition function $Z(t) = \int dx \exp[-H(x,t)/(k_B T)]$ is finite for all $k_B T \geqslant 0$ (k_B denotes the Boltzmann constant). This class of Hamiltonians generalizes the well-known "breathing" parabola model [24] for an overdamped particle trapped in a parametrically driven harmonic potential. It also includes semiclassical two-level (or multilevel) systems with controlled gaps between the individual energy levels [16], and quantum spins, where the control parameter is an externally controlled magnetic field [17].

We connect the system to a heat bath and periodically alter its temperature $T(t)$ with the same finite period t_p as $\lambda(t)$. The parameters under experimental control are thus $\lambda(t)$ and $T(t)$ and our aim is to find optimal t_p-periodic protocols for them under the experimentally motivated constraints [48]

$$\lambda(t) \in [\lambda_-, \lambda_+], \quad T(t) \in [T_-, T_+]. \tag{2}$$

III. MAXIMUM-EFFICIENCY PROTOCOL

Our first main result is a general geometric proof that the maximum-efficiency finite-time cycle under the constraints (2) is a Carnot-Otto cycle composed of two isotherms/isochores interconnected by two adiabats. The maximum-efficiency protocol $\{T(t), \lambda(t)\}$ is thus piecewise constant:

$$\{T(t), \lambda(t)\}_\eta = \begin{cases} \{T_+, \lambda_+\}, & 0 < t < t_+, \\ \{T_-, \lambda_-\}, & t_+ < t < t_p. \end{cases} \tag{3}$$

And the maximum efficiency is given by

$$\eta = 1 - \frac{\lambda_-}{\lambda_+}. \tag{4}$$

The proof relies just on the definition of heat and it is thus independent of the details of the system dynamics, including the times t_+ and t_p. It holds both for situations when the heat bath is memoryless (Markovian) and non-Markovian. The nonequilibrium dynamics of the system communicating with a Markovian bath can be described by Fokker-Planck or master equations for the probability density for x [49]. Except for a few exactly solvable settings [16,49], these equations are usually hard to solve analytically for non-quasi-static time-dependent protocols. However, in the non-Markovian case, a corresponding closed deterministic description might not be available at all [50]. Then one has to resort to stochastic descriptions, such as a generalized Langevin equation, making even a numerical optimization challenging. The derivation also holds in situations with a nonequilibrium bath, such as in recently intensely studied cyclic active Brownian heat engines [51–54].

Let us now derive Eqs. (3) and (4). Under reasonable assumptions, any periodic variation of the control parameters eventually induces a periodic average response of the system, $\sigma(t) = \langle f[x(t)] \rangle$. This ensemble average is a functional of $T(t)$ and $\lambda(t)$ specified by dynamical equations of the system. Due to the factorized structure of the Hamiltonian (1), the average internal energy of the system $\langle H(x,t) \rangle$ is given by $\lambda(t)\sigma(t)$. Decomposing its infinitesimal change into a component corresponding to the external variation of the control λ (work) and the rest (heat) [5,6], it follows that output work and input heat increments are given by $đW_{\text{out}}(t) = -\sigma(t) d\lambda(t)$ and $đQ(t) = \lambda(t) d\sigma(t)$, respectively. Per cycle, the engine transforms the fraction

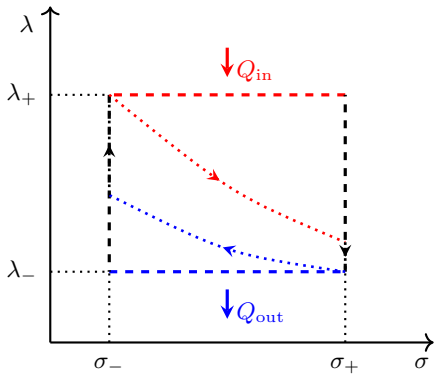

FIG. 1. The maximum-efficiency protocol (3) under the constraints in Eq. (2) (dashed line) compared to a suboptimal cycle (dotted line).

$$\eta = \frac{W_{\text{out}}}{Q_{\text{in}}} = 1 - \frac{Q_{\text{out}}}{Q_{\text{in}}} \tag{5}$$

of the heat

$$Q_{\text{in}} = \int_0^{t_p} \lambda(t) \theta[d\sigma(t)] d\sigma(t) \tag{6}$$

from the heat source into output work

$$W_{\text{out}} = -\int_0^{t_p} \sigma(t) d\lambda(t), \tag{7}$$

and dumps the remaining heat $Q_{\text{out}} = Q_{\text{in}} - W_{\text{out}} = \int_0^{t_p} \lambda(t) \theta[-d\sigma(t)] d\sigma(t)$ into the heat sink. [The Heaviside step function $\theta(\bullet) = 1$ when the heat flows on average into the system, i.e., $d\sigma > 0$.]

Consider now the λ-σ diagram of the cycle depicted in Fig. 1. We seek the shape of the cycle which yields maximum efficiency η under the constraints (2).[1] The cycle must run clockwise to secure that $Q_{\text{in}} > Q_{\text{out}}$. Next, we note that maximizing η amounts to minimizing the ratio $Q_{\text{out}}/Q_{\text{in}}$. For given boundary values $\sigma_\pm$ of σ, this is obviously achieved by setting $\lambda = \lambda_+$ when $d\sigma > 0$ and $\lambda = \lambda_-$ when $d\sigma < 0$. In such a case, $Q_{\text{in}} = \lambda_+ \Delta\sigma$, $Q_{\text{out}} = \lambda_- \Delta\sigma$, and the efficiency is given by Eq. (4). The increase in the system response $\Delta\sigma = \sigma_+ - \sigma_-$, which can be a complicated functional of the protocol $\{T(t), \lambda(t)\}$, canceled out. Equation (4) is thus valid for arbitrary $\sigma_\pm$, and it represents the maximum efficiency of a heat engine based on Hamiltonian (1) under the constraints (2). The corresponding maximum-efficiency protocol for λ forms a rectangle ranging from λ_- to λ_+ in the λ-σ diagram regardless the cycle duration and dynamical equations of the

[1] A similar optimization problem is often solved in courses on classical thermodynamics to show that maximum efficiency of an equilibrium cycle under the constraint $T(t) \in [T_-, T_+]$ on the bath temperature is the Carnot efficiency. However, in our case, the system can be arbitrarily far from equilibrium.

system. The only constraint on these control parameters is that the cycle runs in the λ-σ diagram clockwise.

When not driven, a system out of equilibrium relaxes towards the equilibrium state corresponding to the instantaneous values of the fixed control parameters. For cyclically varied control parameters, the system can no longer relax to equilibrium and its nonequilibrium state "lags behind" the quasistatic cycle specified by the instantaneous values of the control parameters. In our setting, $\sigma(t)$ lags behind $\sigma^{\rm eq}(t) = \int dx f(x) \exp\{-\lambda(t) f(x)/[k_{\rm B} T(t)]\}/Z(t)$. In Appendix B 1, we show that $\sigma^{\rm eq}(t)$ is a monotonically increasing function of T/λ. Denoting as t_+ the duration of the $\lambda = \lambda_+$ branch, clockwise cycles with $\Delta\sigma > 0$ are thus obtained for temperature protocols $T(t)$ which obey (i) $\dot{T}(t) \geqslant 0$ when $\lambda = \lambda_+$, (ii) $\dot{T}(t) \leqslant 0$ when $\lambda = \lambda_-$, and (iii) $T(t_+-)/\lambda_+ > T(t_{\rm p}-)/\lambda_-$, where $T(t-) \equiv \lim_{\epsilon\to 0} T(t - |\epsilon|)$. The last condition implies that the maximum efficiency (4) obeys the standard second-law inequality $\eta \leqslant 1 - T(t_{\rm p}-)/T(t_+-) \leqslant 1 - T_-/T_+$. It saturates for the "compression ratio" $\lambda_-/\lambda_+ = T_-/T_+$. Even for a finite cycle time $t_{\rm p}$, output power, in this case, vanishes because $\sigma^{\rm eq}(t)$ becomes constant, yielding an infinitesimal quasistatic cycle with a vanishing output work. In the maximum-efficiency protocol (3), we use the specific protocol for $T(t)$ that maximizes the upper bound on η. In Appendix B 1, we argue that this temperature protocol also maximizes the output work of the engine regardless of $\lambda(t)$ because it yields the largest temperate differences between the bath and the system when they exchange heat. However, we reiterate that the maximum efficiency (4) can be achieved for an arbitrary protocol for $T(t)$ that obeys the above conditions (i)-(iii). This freedom in $T(t)$ can be exploited in setups where precise control of the bath (effective) temperature is difficult, such as in active Brownian heat engines [52].

The adiabatic branches connecting the isotherms in the protocol (3) can be realised using several qualitatively different approaches [31]. (i) One can disconnect the system from the heat bath, which might be impractical for microscopic engines. (ii) One may keep the system in thermal contact with the bath and vary the control parameters T and λ in such a way that the response σ does not change [55]. This approach allows circumventing some of the shortcomings of overdamped thermodynamics [56], where the heat fluxes through the momentum degrees of freedom are neglected. (iii) One can realize the adiabatic branches by changing the control parameters much faster than the relaxation time of the response σ [57]. In the specific maximum-efficiency protocol (3), we employ the last possibility. It minimizes the cycle time $t_{\rm p}$ and thus maximize the output power $P \equiv W_{\rm out}/t_{\rm p}$. Besides, it allows for a direct comparison with the maximum-efficiency protocols derived for Brownian heat engines under constraints on σ [24]. However, other realisations of the adiabatic branches yield the same maximum efficiency (4). We reiterate that also the choice of the durations t_+ and $t_{\rm p} - t_+$ of the isotherms in (3) do not affect the maximum η.

IV. MAXIMUM-POWER PROTOCOL

If the durations of the isotherms are long enough compared to the relaxation time of the system, i.e., $\Delta\sigma$ is close to its equilibrium value, and the compression ratio λ_-/λ_+ is large, the maximum-efficiency protocol (3) also yields maximum output work $W_{\rm out}$ (7) and power

$$P = \frac{W_{\rm out}}{t_{\rm p}} \tag{8}$$

under the constrained control (2). This is our second main result. To prove it, consider the generally unreachable geometric loose upper bound on the output work $\max W_{\rm out} = \Delta\lambda \max \Delta\sigma^{\rm eq} = (\lambda_+ - \lambda_-)[\sigma^{\rm eq}(T_+/\lambda_-) - \sigma^{\rm eq}(T_-/\lambda_+)]$, which follows from the broadly valid assumption $\max \Delta\sigma < \max \Delta\sigma^{\rm eq}$ and the insight that $W_{\rm out}$ is given by the area enclosed by the cycle in the λ-σ diagram. Expanding $\max W_{\rm out}$ in $\Delta\lambda$ yields $\max W_{\rm out} = \Delta\lambda[\sigma^{\rm eq}(T_+/\lambda_+) - \sigma^{\rm eq}(T_-/\lambda_-)] + \mathcal{O}(\Delta\lambda^2)$. Up to the leading order in $\Delta\lambda$ and under the condition that the system has relaxed at the ends of the two isotherms to equilibrium, this upper bound is saturated by the protocol (3), which completes the proof. We note that (i) the condition $\Delta\sigma = \Delta\sigma^{\rm eq}$ does not mean that the cycle is slow as the system has to be close to equilibrium at the ends of the two isotherms only and can be arbitrarily far from equilibrium otherwise. (ii) This condition allows one to analytically calculate the whole probability distribution for the output work regardless of additional details of the system dynamics [16,58]. Interestingly, for semiclassical systems, piecewise constant protocols with two or more branches also maximize output power when the cycle time is much shorter than the system relaxation time [34,35,59].

Beyond these regimes, $W_{\rm out}$ and P strongly depend on all details of the dynamics through $\sigma(t)$ and cycle time $t_{\rm p}$. While $W_{\rm out}$ and P are still optimized by the temperature protocol and the choice of fast adiabats in (3), optimal protocols for $\lambda(t)$ under the constraints (2) are no longer piecewise constant and they have to be identified for each system separately. Similarly to the derivation of maximum-efficiency and maximum-power protocols under constraints on the system state [24,42–44], this often involves functional optimization or extensive numerical work which are both nontrivial tasks.

In the next section, we illustrate the main features of maximum-efficiency and maximum-power protocols under constrained control on an engine based on an overdamped Brownian particle in a harmonic potential. This model describes experimental realizations of microscopic heat engines using optical tweezers [57,60,61]. Besides, the corresponding maximum-efficiency and maximum-power protocols under the constrained response are known [24], allowing for a direct comparison with our results obtained under constrained control.

V. CASE STUDY: OVERDAMPED BROWNIAN HEAT ENGINE

Let us now consider the specific Brownian heat engine based on an overdamped particle with mobility μ diffusing in a controlled harmonic potential. The Hamiltonian (1) now reads $H(x,t) = \lambda(t)x^2/2$, with x the position of the particle. The response of the system $\sigma(t) = \langle x^2/2\rangle$ is proportional to the position variance and it obeys the first-order differential equation [16,24,62]

$$d\sigma(t)/dt = -2\mu\lambda(t)\sigma(t) + \mu k_{\rm B} T(t). \tag{9}$$

TABLE I. Considered classes of protocols with free parameters a, b, c, d to be determined by the optimization (protocols $\lambda_{\rm pwc}$ and $\lambda_{\rm S}$ have only two free parameters). The protocols are in general discontinuous at times t_+ and $t_{\rm p}$. The piecewise constant protocol $\lambda_{\rm pwc}(t)$ is a variant of the maximum-efficiency protocol $\lambda_\eta(t)$ (3), where $\lambda_{\rm pwc}(t)$ does not have to reach the boundary values λ_- and λ_+. The piecewise linear protocol $\lambda_{\rm pwl}(t)$ has zero curvature. The protocol $\lambda_{\rm slow}(t)$ minimizes the irreversible losses during isothermal branches under close-to-equilibrium conditions. Such protocols can be derived for Brownian heat engines with Hamiltonians of the form $\lambda(t)x^n/n$ (for details, see Appendix C). The protocol $\lambda_{\rm S}(t)$ maximizes both power and efficiency under the constraint that $\sigma(0) = \sigma(t_{\rm p}) \equiv a$ and $\sigma(t_+) \equiv b$ [24]. The corresponding response $\sigma_{\rm S}(t)$ is given by Eq. (D2). For $b = d = 0$, $\lambda_{\rm pwl}$ and $\lambda_{\rm slow}$ reduce to $\lambda_{\rm pwc}$.

	$\lambda_{\rm pwc}(t)$	$\lambda_{\rm pwl}(t)$	$\lambda_{\rm slow}(t)$	$\lambda_{\rm S}(t)$
$t < t_+$	a	$a + bt$	$\frac{a}{(1+bt)^2}$	$\frac{T_+}{2\sigma_{\rm S}(a,b,t)} - \frac{\sqrt{b}-\sqrt{a}}{\mu t_+\sqrt{\sigma_{\rm S}(a,b,t)}}$
$t > t_+$	c	$c + dt$	$\frac{c}{(1+dt)^2}$	$\frac{T_-}{2\sigma_{\rm S}(a,b,t)} + \frac{\sqrt{b}-\sqrt{a}}{\mu t_-\sqrt{\sigma_{\rm S}(a,b,t)}}$

In Sec. III, we proved that the maximum-efficiency protocol under the constraints (2) should, in this case, be the protocol (3). In this section, we illustrate this results by direct numerical optimization. In addition, we ask which protocol for λ yields the largest output power under the constraints (2). Even though the model (9) is exactly solvable [16], the corresponding optimal $\lambda(t)$ has to be found numerically, e.g., by the method in Ref. [63]. To keep the optimization transparent, we instead consider the specific set of families of protocols for the isothermal strokes in Table I and numerically optimize over their free parameters. When such classes are chosen suitably, the resulting suboptimal performance will be close to the global optimum [64,65]. Besides, we use the protocol for temperature and adiabatic branches from Eq. (3), and fix the durations of the two isotherms and thus $t_{\rm p}$. The durations can be further optimized once the optimal variation of λ is known. The solutions to Eq. (9) can involve exponentials of very large or small numbers, which can lead to numerical instabilities inducing large losses of precision, and thus they have to be treated with care. To secure that our solutions are always precise enough, we have solved Eq. (9) in our analysis also numerically.

For the protocols in Table I and the temperature protocol in Eq. (3), we thus numerically optimized the efficiency (5) and output power (8) as functions of the parameters $\{a, b, c, d\}$ under constraints on $\lambda(t)$. For constrained response $\sigma(t)$, we additionally verified in Appendix D that the protocol $\lambda_{\rm S}$ obtained from Ref. [24] indeed yields both the maximum power and maximum efficiency.

The results of optimizing efficiency under the constrained control are depicted in Fig. 2. For all of the trial protocols from Table I except for $\lambda_{\rm S}$ the optimal values of parameters b and d were 0. All these protocols thus collapsed to the piecewise constant maximum-efficiency protocol λ_η (3), illustrating our general theoretical result. Notably, the efficiency achieved by the maximum-efficiency protocol is significantly larger than that provided by usage of the protocol $\lambda_{\rm S}$, which gives maximum efficiency under constrained response.

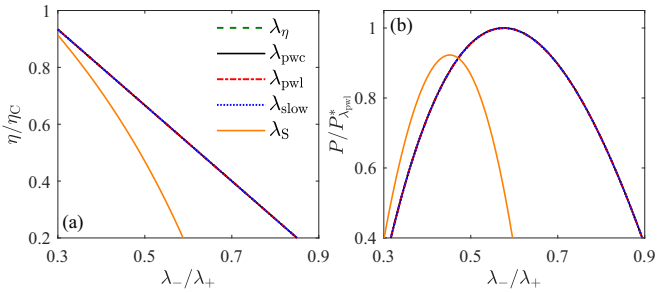

FIG. 2. Numerical optimization of the efficiency of the Brownian heat engine under constrained control verifies that the maximum-efficiency protocol is given by Eq. (3). (a) Maximum efficiency and (b) the corresponding power (in units of the ultimate maximum power $P^*_{\lambda_{\rm pwl}}$ for $\lambda_{\rm pwl}$) as functions of λ_-/λ_+. All protocols except for $\lambda_{\rm S}$ perfectly overlap. Parameters used are $t_+ = t_- = 1$, $k_{\rm B}T_+ = 1$, $k_{\rm B}T_- = 0.25$ (thus Carnot efficiency $\eta_{\rm C} \equiv 1 - T_-/T_+ = 0.75$), $\lambda_+ = 0.5$, and $\mu = 1$.

Main results of the optimization of output power under the constrained control are summarized in Fig. 3. (i) With increasing minimum compression ratio λ_-/λ_+ allowed by the constraints (2), maximum power for all considered protocols in (a) is first constant and then, at an optimal compression ratio r^*, decreases. The decreasing part corresponds to protocols which span between the allowed boundary values, i.e., $\max\lambda(t) = \lambda(0+) = \lambda_+$ and $\min\lambda(t) = \lambda(t_+ +) = \lambda_-$. At the plateau, the boundary values of the protocols are chosen within the bounds (2) to keep the optimal compression ratio r^*. (ii) Values of maximum power obtained for the protocols which have enough free parameters are indistinguishable within our numerical precision. As the corresponding optimized protocols seem to have minimum possible curvature $\ddot{\lambda}(t)$, we conclude that the maximum-power protocol is $\lambda_{\rm pwl}$. (iii) Only the protocol $\lambda_{\rm S}$, optimized for constrained response σ, yields notably smaller power than other protocols. (iv) In agreement with our above discussion, for large enough values of $\lambda_-/\lambda_+ \geqslant 0.59$, the optimized parameters for protocols $\lambda_{\rm pwc}$, $\lambda_{\rm pwl}$, and $\lambda_{\rm slow}$ are $b = d = 0$, $a = \lambda_+$, and $c = \lambda_-$, reducing them to λ_η (3). (v) The maximum powers for the protocols λ_η and $\lambda_{\rm pwl}$ differ just by 1%.

In Fig. 4, we further show that the relative difference in maximum power for $\lambda_{\rm pwl}$ and λ_η is small for a broad range of values of T_-/T_+ and t_-/t_+. From panels (c)–(f) we conclude that the optimal ratio t_-/t_+ is between 1 and 2, which is in agreement with the results of Appendix B 2 b [see Eq. (B19) below]. Thus, for branch durations that optimize output power, the relative difference δP in (a) is always below 12%, decreasing with the temperature ratio. These results indicate that when one can optimize $W_{\rm out}$ and P over λ_-, the maximum-efficiency protocol (3) often yields almost the maximum power.

The optimization over λ_- is natural for experimental platforms with limitations on the maximum strength of the potential only. The maximum power regime of the maximum-efficiency protocol (3) can be, to a large extend, investigated analytically. First, assuming again that durations of the isotherms are long enough that the system is close to equilibrium at times t_+ and $t_{\rm p}$, we have $W_{\rm out} =$

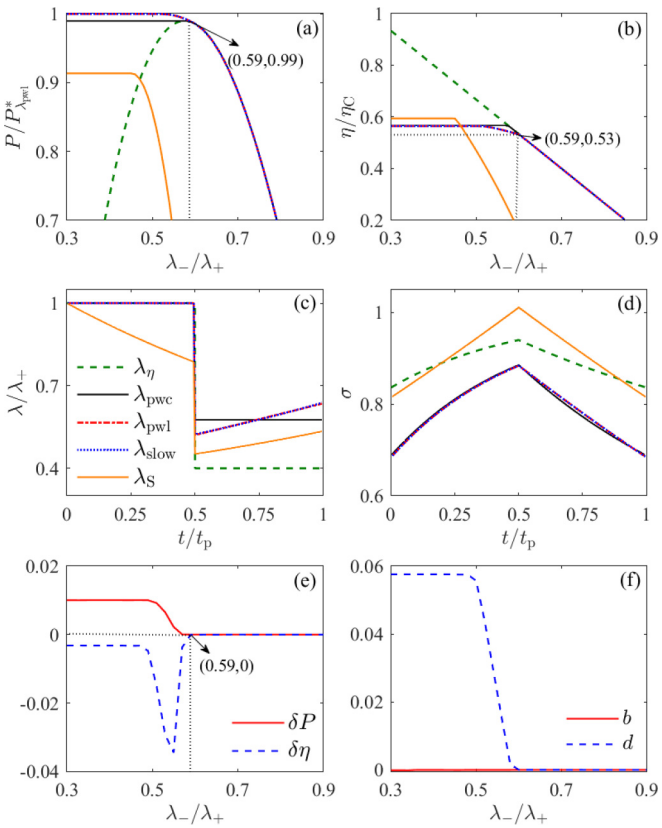

FIG. 3. Numerical optimization of the output power of the Brownian heat engine illustrates that the maximum-efficiency protocol λ_η (3) also yields maximum power when the compression ratio λ_-/λ_+ is large and the durations $t_+ = t_- = 1$ of the two isotherms are comparable to the relaxation times $1/(2\mu\lambda_\pm)$ for σ. (a) Powers (in units of the ultimate maximum power $P^*_{\lambda_{\rm pwl}}$ for $\lambda_{\rm pwl}$) and (b) the corresponding efficiencies obtained using λ_η (3) and the protocols in Table I. For $\lambda_-/\lambda_+ \geqslant 0.59$ all protocols except for λ_S coincide. (c) and (d) show the protocols and the resulting response for $\lambda_-/\lambda_+ = 0.4$. (e) The relative differences $\delta X = (X_{\lambda_{\rm pwl}} - X_{\lambda_{\rm pwc}})/X_{\lambda_{\rm pwl}}$ of power ($X = P$) and efficiency ($X = \eta$) for $\lambda_{\rm pwl}$ and $\lambda_{\rm pwc}$. (f) The optimal values of parameters b and d for $\lambda_{\rm pwl}$. We used the same parameters as in Fig. 2.

$(\lambda_+ - \lambda_-)[\sigma^{\rm eq}(T_+/\lambda_+) - \sigma^{\rm eq}(T_-/\lambda_-)]$. For $f(x) = |x|^n$ in Eq. (1), we then find that the optimal compression ratio is $\lambda_-/\lambda_+ = \sqrt{T_-/T_+}$, which leads to the output work $W_{\rm out} = k_{\rm B}T_+(2\eta_{\rm CA} - \eta_{\rm C})/n$ and Curzon-Ahlborn efficiency $\eta = \eta_{\rm CA} = 1 - \sqrt{T_-/T_+}$ (see Appendix B 2 a for details). For other than power-law Hamiltonians, the efficiency at maximum power can differ from $\eta_{\rm CA}$ but it can still be determined numerically regardless details of dynamical equations for the system (for details, see Appendix B 2 a). Relaxing the assumption of slow (but not quasistatic) isotherms, the optimization of $W_{\rm out}$ with respect to λ_- requires specification of the dynamics. In Fig. 5, we show that the efficiency at maximum power of the Brownian heat engine described by Eq. (9) and driven by the maximum-efficiency protocol (3) is bounded between the Curzon-Ahlborn efficiency, achieved for slow isotherms, and the efficiency $2 - \sqrt{4 - 2\eta_{\rm C}} < \eta_{\rm CA}$, reached in the limit $t_{\rm p} \to 0$.

In closing this section, we summarize the strong effects of the constraints (constrained control versus constrained response [24]). First, constraining the control allowed us to derive much more generally valid results than constraining the response. Second, for the constrained response, the power and efficiency can be optimized simultaneously, whereas for the constrained control this is, in general, not possible. Third, the resulting functional forms of the optimal protocols and the corresponding optimal performance strongly differ. Fourth, the change of boundary conditions alters the optimal allocation of cycle duration between hot and cold isotherms, t_+/t_-, as we show below Eq. (B19) in the Appendix.

VI. CONCLUSION

We have optimized the thermodynamic performance of finite-time overdamped stochastic heat engines under the constraint that control parameters, such as potential strength or bath temperature, can be varied only over a limited range. This optimization problem is experimentally motivated and differs from previously studied optimization studies performed with constraints on the system's state. We have found that, for working fluids described by the experimentally most common "breathing" Hamiltonians proportional to a control parameter, the maximum efficiency is reached by piecewise constant modulation of the control parameters, independently of the detailed dynamics of the system. When the control parameter can only be changed over a small range and the system is close to equilibrium at the ends of the isotherms, the maximum-efficiency protocol also yields maximum output power. But outside this regime, the maximization of power requires specifying the dynamical equations of the working fluid. For engines based on an overdamped Brownian particle trapped in a harmonic potential, we numerically found that the maximum-power protocol is linear. Nevertheless, the global maxima of the maximum-power and maximum-efficiency protocols are in this setting close, suggesting that the maximum-efficiency protocol provides a reasonable estimate of the output power.

The main strength of the presented derivations of the maximum-efficiency and maximum-power protocols under constrained control is their simplicity and unprecedented generality. Their possible extension to more complicated Hamiltonians is sketched in Appendix A. While more general extensions remain to be explored in future work, the validity of our results for Brownian heat engines is already of experimental relevance. These engines are often realized using optical tweezers with strict bounds on the trap stiffness λ: too small λ leads to losing the Brownian particle while too large λ can induce its overheating. Interestingly, the achievable trap stiffnesses are well above 10^{-6} N/m [31]. For spherical Brownian particles with the radius of 10^{-6} m in water, the Stokes law predicts the mobility of $\mu \approx 0.5 \times 10^8$ m/Ns, leading to the relaxation time $1/(2\mu\lambda)$ of the response σ on the order of 10^{-2} s. The assumption that the durations of the isotherms are longer than the response relaxation time, used in our derivation of the maximum-power protocol, is thus, in this setup, natural. Besides, we believe that extensions of our results can find applications in more involved optimization tasks, e.g., performed using machine learning algorithms [66,67] or geometric methods [68,69], as well as in quantum setups [39,70,71].

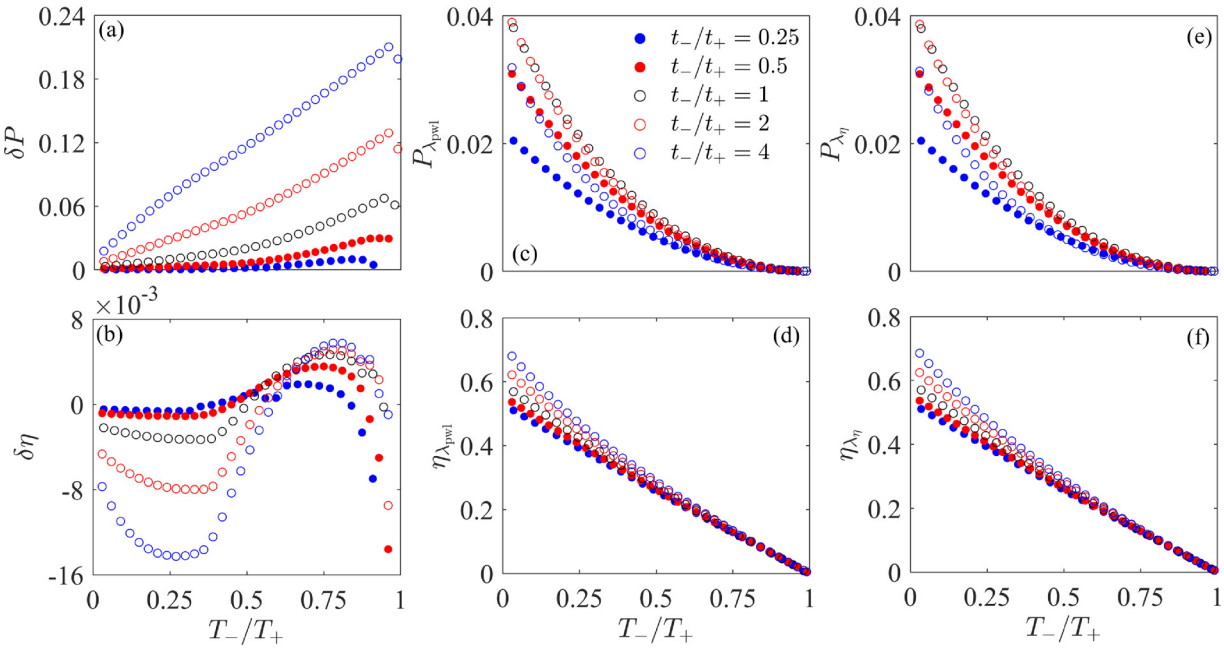

FIG. 4. The relative differences $\delta X = (X_{\lambda_{\rm pwl}} - X_{\lambda_\eta})/X_{\lambda_{\rm pwl}}$ of (a) maximum power ($X = P$) optimized with respect to λ_- and (b) the corresponding efficiency ($X = \eta$) for the linear protocol $\lambda_{\rm pwl}$ and the maximum-efficiency protocol (3) for different values of T_-/T_+ and t_-/t_+. (c)–(f) show the corresponding values of maximum power and efficiency. The piecewise constant protocol $\lambda_{\rm pwc}$ and the maximum-efficiency protocol λ_η (3) are in this case equal. We used the same parameters as in Fig. 2.

ACKNOWLEDGMENTS

Z.Y. is grateful for the sponsorship of China Scholarship Council (CSC) under Grant No. 201906310136. F.C. gratefully acknowledges funding from the Fundational Questions Institute Fund (FQXi-IAF19-01). P.A. is supported by la Caixa Foundation (ID 100010434, Grant No. LCF/BQ/DI19/11730023), and by the Government of Spain (FIS2020-TRANQI and Severo Ochoa CEX2019-000910-S), Fundacio Cellex, Fundacio Mir-Puig, Generalitat de Catalunya (CERCA, AGAUR SGR 1381. J.A. acknowledges funding from the Engineering and Physical Sciences Research Council (EPSRC) (EP/R045577/1) and thanks the Royal Society for support. M.P.L. acknowledges financial support from the Swiss National Science Foundations (Ambizione Grant No. PZ00P2-186067). V.H. gratefully acknowledges support by the Humboldt foundation and by the Czech Science Foundation (Project No. 20-02955J).

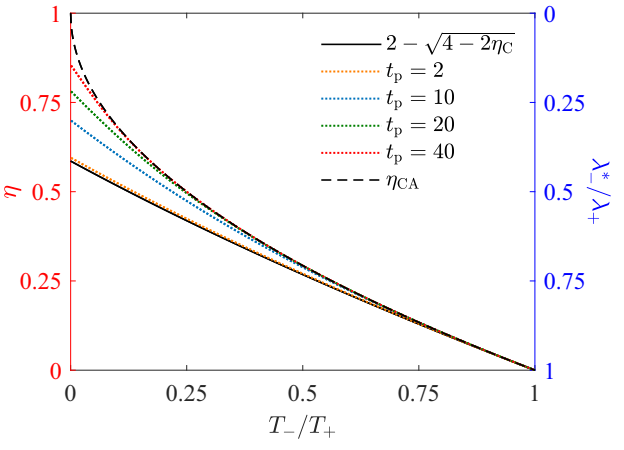

FIG. 5. Efficiency at maximum output power (η, red axis) and the corresponding optimal compression ratio (λ_-^*/λ_+, blue axis) for the maximum-efficiency protocol (3) as functions of the temperature ratio T_-/T_+ for six values of cycle duration $t_{\rm p}$ (colored curves) and $t_- = t_+$. The cycle time, $t_{\rm p}$, is measured in units of the system relaxation time during the hot isotherm. The corresponding ratio during the cold isotherm reads $t_{\rm p}\,\lambda_-^*/\lambda_+$. We used the same parameters as in Fig. 2.

APPENDIX A: MAXIMUM-EFFICIENCY PROTOCOL FOR MULTITERM HAMILTONIANS

Consider a heat engine with a working fluid described by the Hamiltonian

$$H(x,t) = \sum_i \lambda_i(t) f_i(x) \tag{A1}$$

with control parameters $\lambda_i(t)$, $i = 1, \ldots, N$. As in the main text, we now aim to derive the finite-time protocol for the constrained control parameters, $\lambda_i(t) \in (\lambda_i^-, \lambda_i^+)$, which would yield maximum efficiency of the engine. It will turn out that if the compression ratios λ_i^-/λ_i^+ for all the control parameters equal, the geometric argument from the main text still applies.

The heat increment is for the Hamiltonian (A1) given by $đQ = \sum_i \lambda_i(t) d\sigma_i(t)$ with the response functions $\sigma_i(t) = \langle f_i(x) \rangle$. For arbitrary fixed maximum changes $\Delta\sigma_i$ in the response functions during the cycle, geometric upper and lower bounds on $Q_{\rm in}$ and $Q_{\rm out}$ and thus on efficiency are achieved by clockwise rectangular cycles in the individual λ_i-σ_i diagrams. These hypothetical cycles yield the following geometric upper

bound on efficiency:

$$\eta = 1 - \frac{Q_{\rm out}}{Q_{\rm in}} \leqslant 1 - \frac{\sum_i \Delta\sigma_i \lambda_i^-}{\sum_i \Delta\sigma_i \lambda_i^+}. \tag{A2}$$

We use the term "geometric" to stress that this bound follows from the analysis of the cycle in the λ-σ diagram, without considering the relation between the protocol $[\lambda_1(t), \ldots, \lambda_N(t)]$ and the response $[\sigma_1(t), \ldots, \sigma_N(t)]$ imposed by dynamical equations of the working fluid. This means that the given set of $\Delta\sigma_i$ might not be achievable by the piecewise constant protocol and thus the bound in (A2) is loose. Furthermore, we seek an optimal protocol constrained just by the conditions on λ_i, and the upper bound in (A2) in general strongly depends on the fixed values of $\Delta\sigma_i$. For the single-term Hamiltonian $H(x,t) = \lambda(t) f(x)$ used in the main text, this has not been an issue because then $\Delta\sigma$ in the nominator and denominator in (A2) cancel out and the upper bound becomes independent of the details of the dynamics. The optimal protocol for efficiency is then the piecewise constant protocol for $\lambda(t)$ because it saturates the geometric upper bound. To sum up, the bound in (A2) allows one to derive the maximum-efficiency protocol only if it happens to be independent of $\Delta\sigma_i$. In the opposite case, the optimal protocol cannot be determined without considering the dynamical equations and performing the corresponding functional optimization.

Let us now investigate when the upper bound in (A2) becomes independent of the system response, $\Delta\sigma_i$. Defining the set of "probabilities" $p_i = \Delta\sigma_i \lambda_i^+ / \sum_i \Delta\sigma_i \lambda_i^+$, the ratio in the upper bound in (A2) can be rewritten as the average

$$\frac{\sum_i \Delta\sigma_i \lambda_i^-}{\sum_i \Delta\sigma_i \lambda_i^+} = \sum_i p_i \frac{\lambda_i^-}{\lambda_i^+}. \tag{A3}$$

This expression becomes independent of σ_i only if all the compression ratios λ_i^-/λ_i^+ are equal. In such a case, the maximum-efficiency protocol is thus a piecewise constant protocol for each of λ_i and yields the efficiency

$$\eta = 1 - \lambda_i^-/\lambda_i^+. \tag{A4}$$

Besides this result, the probabilistic interpretation (A3) of the upper bound in (A2) also yields the dynamics independent (but in general loose) *upper bound* on efficiency,

$$\eta \leqslant 1 - \min_i \frac{\lambda_i^-}{\lambda_i^+}. \tag{A5}$$

To close this section, we note that a piecewise constant protocol for λ_i will always yield the efficiency $1 - (\sum_i \Delta\sigma_i \lambda_i^-)/(\sum_i \Delta\sigma_i \lambda_i^+)$, with values of $\Delta\sigma_i$ induced by the dynamical equations of the system. Within the class of piecewise constant protocols, the upper bound (A5) is then tight if the constraints on all the control parameters λ_i allow to achieve the minimum compression ratio $\min_i \frac{\lambda_i^-}{\lambda_i^+}$. Furthermore, for such protocols, Eq. (A3) also implies the *lower bound* on the efficiency,

$$\eta \geqslant 1 - \max_i \frac{\lambda_i^-}{\lambda_i^+}, \tag{A6}$$

which is always tight.

APPENDIX B: PROPERTIES OF MAXIMUM-EFFICIENCY PROTOCOL

In this section, we provide further details concerning the maximum-efficiency protocol for the Hamiltonian, $H(x,t) = \lambda(t) f(x)$, discussed in the main text. First, we argue that the maximum-efficiency protocol that yields maximum output work for the given piecewise constant $\lambda(t)$ requires piecewise constant variation of temperature. Then, we investigate output power of the maximum-efficiency protocol as a function of the lower bound on the control parameter $\lambda(t)$.

1. Temperature protocol

In the main text, we have shown that the maximum-efficiency protocol for the control parameter $\lambda(t)$ is piecewise constant and the corresponding efficiency $\eta = 1 - \lambda_-/\lambda_+$. The only condition on the temperature protocol was that the cycle is performed clockwise in the λ-σ diagram. Nevertheless, in order to allow the engine to operate at Carnot efficiency and to maximize its output work, we have chosen the protocol (3).

For this choice of $T(t)$, the working medium of the engine operates with the largest possible temperature gradient during the whole cycle. This maximizes the heat flux through the engine, which can be utilized to yield the maximum amount of work $W_{\rm out} = \eta Q_{\rm in}$. Besides, the engine efficiency η is also known to increase with the bath temperature difference [see also Figs. 4(c)–4(f)].

Let us now provide an alternative and more technical argument that the choice of $T(t)$ in Eq. (3) maximizes the output work. We restrict this argument to the maximum-efficiency protocol for λ in Eq. (3). However, generalizations to other protocols are straightforward. The main idea is that connecting the system to the hottest possible bath when $\dot\sigma > 0$ and to the coldest possible bath when $\dot\sigma < 0$ maximizes the extent of the cycle in the σ direction in the σ-λ diagram and thus also $W_{\rm out}$.

For the protocol (3), the output work is given by

$$W_{\rm out} = \Delta\lambda \Delta\sigma, \tag{B1}$$

with $\Delta\lambda = \lambda_+ - \lambda_-$ and the maximum change in the response parameter during the cycle $\Delta\sigma = \sigma_+ - \sigma_-$. To maximize $W_{\rm out}$, we thus need to maximize $\Delta\sigma$. To this end, it is reasonable to assume that

$$\Delta\sigma \leqslant \Delta\sigma^{\rm eq}, \tag{B2}$$

where $\Delta\sigma^{\rm eq} = \max \sigma^{\rm eq} - \min \sigma^{\rm eq}$ is the maximum change in the response parameter σ during the cycle with isochoric branches (constant λ) longer than the system relaxation time. This assumption is in particular valid for arbitrary overdamped dynamics, where σ always converges to its equilibrium value ($k_{\rm B}$ denotes the Boltzmann constant)

$$\sigma^{\rm eq}(t) = \sum_x f(x) \frac{\exp\{-\lambda(t) f(x)/[k_{\rm B} T(t)]\}}{\sum_x \exp\{-\lambda(t) f(x)/[k_{\rm B} T(t)]\}}, \tag{B3}$$

corresponding to the instantaneous values of the control parameters $\{T(t), \lambda(t)\}$. Noticing that $\sigma^{\rm eq}(t) = U(t)/\lambda(t)$, where $U(t) = \langle H(x,t)\rangle$ is the thermodynamic internal energy

of the system, the positivity of heat capacity

$$C_{\rm v} = \frac{\partial U}{\partial T} = \frac{\partial \sigma^{\rm eq}}{\partial (T/\lambda)} > 0 \tag{B4}$$

implies that $\sigma^{\rm eq}$ is a monotonously increasing function of the ratio T/λ.

From Fig. 1 in the main text, it follows that $\max \sigma^{\rm eq}$ and $\min \sigma^{\rm eq}$ are the values of $\sigma^{\rm eq}$ at the ends of the isochores with $\lambda = \lambda_+$ and $\lambda = \lambda_-$, respectively. The upper bound on $\Delta\sigma$ is thus given by

$$\max \sigma^{\rm eq} - \min \sigma^{\rm eq} = \sigma^{\rm eq}(T_+/\lambda_+) - \sigma^{\rm eq}(T_-/\lambda_-). \tag{B5}$$

It is attained for slow isochores when $T = T_+$ for $\lambda = \lambda_+$ and $T = T_-$ for $\lambda = \lambda_-$. As long as $\dot\sigma^{\rm eq} > 0$ for $\lambda = \lambda_+$ and $\dot\sigma^{\rm eq} < 0$ for $\lambda = \lambda_-$ (so that the used definitions of input and output heat hold), details of the temperature protocol during the isochores in this limit do not alter the value of $\Delta\sigma^{\rm eq}$ and thus $W_{\rm out} = \Delta\lambda\Delta\sigma^{\rm eq}$. However, these details become important for finite-time cycles.

A typical dynamical equation for an overdamped degree of freedom has the form

$$\dot\sigma(t) = t_{\rm R}^{-1}[\sigma^{\rm eq} - \sigma(t)]. \tag{B6}$$

For constant values of control parameters $T(t)$ and $\lambda(t)$, which enter the relaxation time $t_{\rm R}$ and the equilibrium state $\sigma^{\rm eq}(t)$ defined in Eq. (B3), this equation describes an exponential relaxation of σ to $\sigma^{\rm eq}$ (for a specific example, see Sec. B 2 b). For a cyclic variation of the control parameters, σ lags behind $\sigma^{\rm eq}$ [72]. More precisely, $\sigma \leqslant \sigma^{\rm eq}$ and $\dot\sigma \geqslant 0$ for $\lambda = \lambda_+$, when $\sigma^{\rm eq}$ increases to $\max \sigma^{\rm eq}$, and $\sigma \geqslant \sigma^{\rm eq}$ and $\dot\sigma \leqslant 0$ for $\lambda = \lambda_-$, when $\sigma^{\rm eq}$ decreases to $\min \sigma^{\rm eq}$. The change in the response $\Delta\sigma = \int_0^{t_+} \dot\sigma\, dt = -\int_{t_+}^{t_{\rm p}} \dot\sigma\, dt$ and thus it can be maximized by maximizing (minimizing) the instantaneous rate of change of the response, $\dot\sigma$, during the first (second) isochore. From Eq. (B6), it follows that this is achieved by setting $\sigma^{\rm eq} = \max \sigma^{\rm eq}$ during the fist isochore and $\sigma^{\rm eq} = \min \sigma^{\rm eq}$ during the second one. Altogether, this suggests that the piecewise constant temperature protocol in Eq. (3) yields maximum $\Delta\sigma$ and thus output work $W_{\rm out}$ (B1) for arbitrary cycle duration.

2. Efficiency at maximum power

Let us now turn to the task of maximizing the output work $W_{\rm out} = (\lambda_+ - \lambda_-)\Delta\sigma$ with respect to λ_-. Analytical results can be obtained in the limits of slow and fast isotherms.

a. Slow isotherms

When the duration of the isotherms is longer than the relaxation time of the response σ, one can approximate σ_+ and σ_- in $\Delta\sigma$ by their equilibrium values. Using Eq. (B1), the output work then reads

$$W_{\rm out} = \Delta\lambda\Delta\sigma^{\rm eq}. \tag{B7}$$

Equation (B4) implies that the partial derivative of $\sigma^{\rm eq}$ with respect to the control parameter λ (T is constant) is given by

$$\frac{\partial}{\partial\lambda}\sigma^{\rm eq}(T/\lambda) = -\frac{T}{\lambda^2}C_{\rm v}. \tag{B8}$$

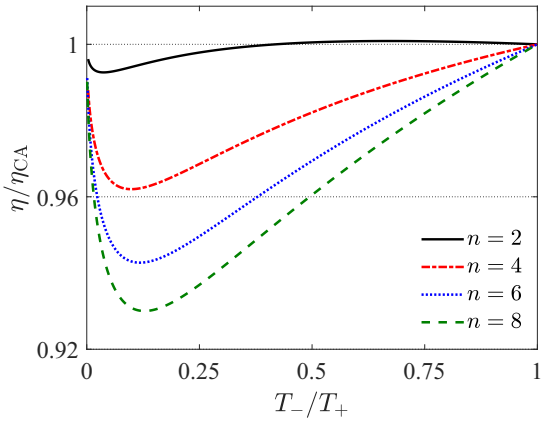

FIG. 6. Efficiency at maximum output work obtained using the Hamiltonian $H = \lambda(t)(|x|^n/n - \ln|x|)$ as a function of T_-/T_+. Parameters used are $k_{\rm B}T_+ = 1$ and $\lambda_+ = 0.5$.

The condition on the extreme of $W_{\rm out}$ (B7) with respect to λ_- thus reads

$$\frac{\partial W_{\rm out}}{\partial\lambda_-} = (\lambda_+ - \lambda_-)\frac{T_-}{\lambda_-^2}C_{\rm v}(T_-/\lambda_-) - \frac{U(T_+/\lambda_+)}{\lambda_+} + \frac{U(T_-/\lambda_-)}{\lambda_-} = 0, \tag{B9}$$

where we additionally used the relation $\sigma^{\rm eq} = U/\lambda$ between $\sigma^{\rm eq}$ and the internal energy U.

For power law Hamiltonians of the form $H = \lambda|x|^n/n$ where $C_{\rm v} = k_{\rm B}/n$ and $U = k_{\rm B}T/n$, this equation can be solved explicitly. The resulting optimal compression ratio is given by $\lambda_-/\lambda_+ = \sqrt{T_-/T_+}$. The corresponding efficiency at the maximum output work is given by the Curzohn-Ahlborn efficiency,

$$\eta = 1 - \frac{\lambda_-}{\lambda_+} = 1 - \sqrt{\frac{T_-}{T_+}} \equiv \eta_{\rm CA}, \tag{B10}$$

and the maximum output work is (Carnot efficiency $\eta_{\rm C} = 1 - T_-/T_+$)

$$W_{\rm out} = \frac{k_{\rm B}T_+}{n}(2\eta_{\rm CA} - \eta_{\rm C}). \tag{B11}$$

Let us now consider the asymmetric Hamiltonian $H = \lambda(t)(|x|^n/n - \ln|x|)$. In this case, the internal energy and heat capacity are given by

$$U = \frac{k_{\rm B}T + \lambda\left[1 + \ln\frac{\lambda}{nk_{\rm B}T} - \psi^{(0)}\left(\frac{\lambda+k_{\rm B}T}{nk_{\rm B}T}\right)\right]}{n}, \tag{B12}$$

$$C_{\rm v} = \frac{nk_{\rm B}T(k_{\rm B}T - \lambda) + \lambda^2\psi^{(1)}\left(\frac{\lambda+k_{\rm B}T}{nk_{\rm B}T}\right)}{n^2k_{\rm B}^2T^2}, \tag{B13}$$

where $\psi^{(m)}(z)$ denotes the polygamma function of order m. In this case, Eq. (B9) is transcendental and we solved it numerically. In Fig. 6, we show the resulting efficiency at the maximum output work as a function of T_-/T_+. Even though the resulting efficiency is still close to $\eta_{\rm CA}$, it can be both slightly larger and smaller than that.

b. Fast isotherms

Let us now assume that the duration of the isothermal branches are much shorter than the system relaxation time. In such a case, the work optimization cannot be done without specifying the dynamical equation for the response σ. To this end, we assume that it obeys the overdamped equation (B6) with the equilibrium value $\sigma^{\rm eq}$ and relaxation time t_R determined by the values of the control parameters $\{T(t), \lambda(t)\}$ at time t. The most prominent examples of systems described by this formula are a two-level system [35] and an overdamped particle trapped in a harmonic potential [24].

Solving Eq. (B6) for the maximum-efficiency protocol (3), we find that

$$\sigma(t) = \begin{cases} \sigma_0 e^{-\frac{t}{t_R^+}} + \sigma_{\rm eq}^+\left(1 - e^{-\frac{t}{t_R^+}}\right), & 0 < t < t_+, \\ \sigma_1 e^{-\frac{t-t_+}{t_R^-}} + \sigma_{\rm eq}^-\left(1 - e^{-\frac{t-t_+}{t_R^-}}\right), & t_+ < t < t_{\rm p}, \end{cases} \tag{B14}$$

where $\sigma_0 \equiv \sigma(0)$ and $\sigma_1 \equiv \sigma(t_+)$ are determined by the condition that $\sigma(t)$ must be a continuous function of time. The variables corresponding to the first (second) isotherm are denoted by max (min). It turns out that

$$\begin{aligned} \Delta\sigma &= \sigma_+ - \sigma_- = \sigma_1 - \sigma_0 \\ &= \Delta\sigma^{\rm eq} \frac{\sinh(t_+/t_{\rm R}^+)\sinh(t_-/t_{\rm R}^-)}{\sinh(t_+/t_{\rm R}^+ + t_-/t_{\rm R}^-)} \leqslant \Delta\sigma^{\rm eq}. \end{aligned} \tag{B15}$$

Substituting this result into the expression for the output work (B1) and expanding the result up to the leading order in the ratios of duration of the individual isotherms to the corresponding relaxation times, $t_+/t_{\rm R}^+$ and $t_-/t_{\rm R}^-$, we find that

$$W_{\rm out} = \Delta\lambda\Delta\sigma^{\rm eq} \frac{\frac{t_+ t_-}{t_{\rm R}^+ t_{\rm R}^-}}{\frac{t_+}{t_{\rm R}^+} + \frac{t_-}{t_{\rm R}^-}}. \tag{B16}$$

To maximize the output work, we need to choose a specific model to determine the dependence of the equilibrium values of response and relaxation times on the control parameters. To this end, we consider the paradigmatic model of stochastic thermodynamics, $\dot\sigma(t) = -2\,\mu\,\lambda(t)\,\sigma(t) + \mu\,k_{\rm B}T$, describing an overdamped Brownian particle with mobility μ in a harmonic trap [24,62]. In this case, $\sigma^{\rm eq} = T/(2\mu\lambda)$ and $t_R = 1/(2\mu\lambda)$, and the maximum output work (B16) is produced for

$$\frac{\lambda_-}{\lambda_+} = \sqrt{(\alpha+1)(\alpha+1-\eta_{\rm C})} - \alpha, \tag{B17}$$

where $\alpha \equiv t_+/t_-$. The corresponding efficiency reads

$$\eta = 1 - \frac{\lambda_-}{\lambda_+} = \alpha + 1 - \sqrt{(\alpha+1)(\alpha+1-\eta_{\rm C})}, \tag{B18}$$

which reduces to $\eta_{\rm CA}$ for $\alpha \to 0$ and $\eta_{\rm C}/2$ for $\alpha \to \infty$. Assuming that $\alpha = 1$ ($t_+ = t_-$), Eq. (B18) is given by the formula

$$\eta = 2 - \sqrt{4 - 2\eta_{\rm C}} = \frac{\eta_{\rm C}}{2} + \frac{\eta_{\rm C}^2}{16} + \mathcal{O}\big(\eta_{\rm C}^3\big) \tag{B19}$$

used in the main text. The corresponding expansion for the Curzohn-Ahlborn efficiency, $\eta_{\rm CA} \approx \frac{\eta_{\rm C}}{2} + \frac{2\eta_{\rm C}^2}{16}$, has an identical linear term and a twice larger quadratic term.

Last but not least, with respect to α, the output power $W_{\rm out}/t_{\rm p}$ using Eq. (B16) develops a peak at $\alpha = \alpha^* = \sqrt{\frac{\lambda_-}{\lambda_+}} < 1$. This also contradicts the situation with constrained σ, where maximum power is attained when the durations of the isotherms are equal ($\alpha = \alpha^* = 1$) [24].

APPENDIX C: OPTIMAL DRIVING FOR SYSTEMS CLOSE TO EQUILIBRIUM

In this Appendix, we consider optimization of a slowly driven heat engine based on an overdamped Brownian particle trapped in the power-law potential $H = \lambda(t)x^n/n$ with $n = 2, 4, \ldots$. We use the temperature protocol from Eq. (3) and impose fixed values of the response σ (or, in the slow driving limit equivalently also the control λ) at the ends of the two isotherms. Dynamics of the particle position is described by the Langevin equation

$$\dot x = -\mu\lambda(t)x^{n-1} + \sqrt{2D(t)}\xi(t), \tag{C1}$$

where $D(t) = \mu k_{\rm B}T(t)$ denotes the diffusion coefficient. From Eq. (C1) and its formal solution

$$x(t) = -\mu\int dt\,\lambda(t)x^{n-1}(t) + \sqrt{2D(t)}\int dt\,\xi(t), \tag{C2}$$

we find that $\langle x(t)\xi(t)\rangle = \sqrt{D/2}$ and thus

$$\frac{d}{dt}\langle x^2(t)\rangle = -2\mu\lambda(t)\langle x^n(t)\rangle + 2D. \tag{C3}$$

Let us now assume that the control parameters $\{T(t), \lambda(t)\}$ vary slowly with respect to the relaxation time of the system, such that, during the limit cycle, the system is always close to equilibrium, and solve this equation up to the first order in $\dot\lambda(t)$. To this end, we consider the ansatz $\langle x^2(t)\rangle = \langle x^2(t)\rangle_0$ and $\langle x^n(t)\rangle = \langle x^n(t)\rangle_0 + \langle x^n(t)\rangle_{\dot\lambda}$, where

$$\langle x^m(t)\rangle_0 = \int_{-\infty}^{\infty} dx\,x^m\,\frac{\exp\left(-\mu\frac{\lambda x^n}{nD}\right)}{Z}, \tag{C4}$$

with the partition function $Z = 2[nD/\mu\lambda(t)]^{1/n}\Gamma(1+1/n)$, is the value of the moment $\langle x^m(t)\rangle$ corresponding to the infinitely slow driving, and $\langle x^n(t)\rangle_{\dot\lambda}$ is the correction proportional to $\dot\lambda$. We find that

$$\langle x^n(t)\rangle_0 = \frac{D(t)}{\mu\lambda(t)}, \tag{C5}$$

$$\langle x^2(t)\rangle_0 = \left[\frac{nD(t)}{\mu\lambda(t)}\right]^{2/n}\frac{\Gamma(3/n)}{\Gamma(1/n)}, \tag{C6}$$

and

$$\langle x^n(t)\rangle_{\dot\lambda} = -\frac{1}{2\mu\lambda(t)}\frac{d}{dt}\langle x^2(t)\rangle_0. \tag{C7}$$

We reiterate that this solution is valid only for protocols $\{T(t), \lambda(t)\}$ which are changing slowly with respect to the relaxation time of the system so that the system is, during the whole cycle, close to equilibrium. However, as we know from the previous discussion, both the piecewise constant

maximum-efficiency protocol for constrained control and the optimal protocol (D1) for the constrained response contain discontinuities, where $\{T(t), \lambda(t)\}$ changes abruptly. To be able to use the slow driving approximation for the derivation of optimal cyclic protocols, we thus need to additionally assume that during these jumps the system is not driven far from equilibrium. To this end, we assume that the ratio $\lambda(t)/T(t)$ in the Boltzmann factor is during the jumps at the ends of the isotherms constant. This additional assumption fixes the state of the system σ at the ends of the isotherms and thus the present optimization scheme is only suitable for the optimization under the constrained response. Let us now proceed with the optimization.

Work done on the system during the time interval $t_\mathrm{i} \leqslant t \leqslant t_\mathrm{f}$ for the given Hamiltonian reads

$$W = \frac{1}{n}\int_{t_\mathrm{i}}^{t_\mathrm{f}} dt\, \dot{\lambda}(t)\langle x^n(t)\rangle \equiv W(t_\mathrm{i}, t_\mathrm{f}). \tag{C8}$$

Having fixed the state of the system at the ends of the isotherms, it is enough to maximize the work during these branches. For an isothermal process, the work Eq. (C8) can be written as $W = \Delta F + W_\mathrm{irr}$, where the first term, denoting the nonequilibrium free energy difference [24], comes from $\langle x^n(t)\rangle_0$, and the second term reads

$$W_\mathrm{irr} = \frac{1}{n}\int_{t_\mathrm{i}}^{t_\mathrm{f}} dt\, \dot{\lambda}(t)\langle x^n(t)\rangle_{\dot{\lambda}} = \frac{1}{n^2\mu}\left(\frac{nD}{\mu}\right)^{2/n} \times \frac{\Gamma(3/n)}{\Gamma(1/n)}\int_{t_\mathrm{i}}^{t_\mathrm{f}} dt\, \dot{\lambda}(t)^2\lambda(t)^{-2(1+n)/n}. \tag{C9}$$

As ΔF is fixed by the imposed boundary conditions on the state of the system σ, to maximize the output work $-W$ means to minimize the irreversible work W_irr as a functional of $\lambda(t)$. This leads to the Euler-Lagrange equation

$$\ddot{\lambda}(t)\lambda(t) - \frac{1+n}{n}\dot{\lambda}(t)^2 = 0, \tag{C10}$$

which has the general solution

$$\lambda_\mathrm{slow}(t) = \frac{a}{(1+bt)^n}. \tag{C11}$$

We thus come to an interesting conclusion that the optimal slow protocol for the constrained response scales with the same exponent as the potential. The values of a and b can be expressed in terms of the boundary conditions for $\lambda_\mathrm{slow}(t)$, i.e., $\lambda_\mathrm{slow}(t_\mathrm{i}) \equiv \lambda_\mathrm{i}$ and $\lambda_\mathrm{slow}(t_\mathrm{f}) \equiv \lambda_\mathrm{f}$. The optimal slow protocol (C11) then reads

$$\lambda_\mathrm{slow}(t) = \frac{\lambda(t_\mathrm{i})}{\left[1 + \left(\sqrt[n]{\frac{\lambda(t_\mathrm{i})}{\lambda(t_\mathrm{f})}} - 1\right)\frac{t-t_\mathrm{i}}{t_\mathrm{f}-t_\mathrm{i}}\right]^n}. \tag{C12}$$

And the corresponding irreversible work and input work are given by

$$W_\mathrm{irr} = \frac{\frac{\Gamma(3/n)}{\Gamma(1/n)}\left[\frac{nD}{\mu\lambda_\mathrm{i}}\right]^{2/n}\left(\sqrt[n]{\frac{\lambda_\mathrm{i}}{\lambda_\mathrm{f}}}-1\right)^2}{\mu(t_\mathrm{f}-t_\mathrm{i})}, \tag{C13}$$

$$W = \frac{\frac{\Gamma(3/n)}{\Gamma(1/n)}\left[\frac{nD}{\mu\lambda_\mathrm{i}}\right]^{2/n}\left(\sqrt[n]{\frac{\lambda_\mathrm{i}}{\lambda_\mathrm{f}}}-1\right)^2}{\mu(t_\mathrm{f}-t_\mathrm{i})} - \frac{D}{n\mu}\ln\frac{\lambda_\mathrm{i}}{\lambda_\mathrm{f}}. \tag{C14}$$

These results are valid for the individual isothermal branches of the cycle. Importantly, the obtained optimized values of the irreversible work are correct up to the order $1/(t_\mathrm{f} - t_\mathrm{i})$, which is their exact dependence on the process duration [24]. These results are thus exact even though they were obtained from the approximate optimal protocol. According to Refs. [24,73], these irreversible works determine the optimal performance of the engine under the constrains on σ, i.e., they give the maximum output work $W_\mathrm{out} = -W(0, t_+) - W(t_+, t_p)$ and efficiency $\eta = W_\mathrm{out}/[T_h\Delta S - W_\mathrm{irr}(0, t_+)]$ (ΔS is the increase in entropy of the system during the hot isotherm). Also this performance is thus from the approximate analysis based on the slow driving obtained exactly.

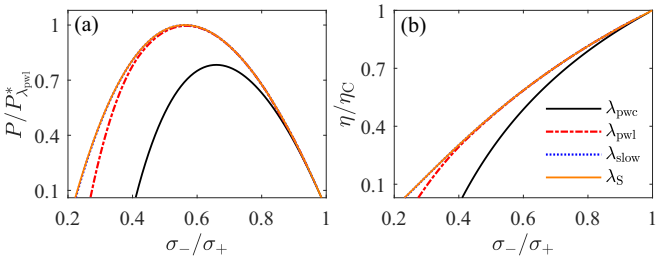

FIG. 7. Optimal performance for fixed boundary values of the response: $\sigma_- \equiv \sigma(0) = \sigma(t_\mathrm{p})$ and $\sigma_+ \equiv \sigma(t_+) = 0.5$. (a) Maximum power (in units of the ultimate maximum power $P^*_{\lambda_\mathrm{pwl}}$ for λ_pwl) and (b) maximum efficiency as functions of σ_-/σ_+. Lines corresponding to λ_S (orange solid) and λ_slow (blue dotted) perfectly overlap. The maximum-efficiency protocol (3) and the piecewise constant protocol λ_pwc are in this case equal. We used the same parameters as in Fig. 2.

APPENDIX D: CONSTRAINED RESPONSE

To test our numerical procedure, in this Appendix we check numerically that the protocol λ_S obtained from Ref. [24] is indeed optimal for both power and efficiency under the constraints on σ. When the values of the response (position variance) σ at the ends of the two isotherms are fixed, i.e., $\sigma_- \equiv \sigma(0) = \sigma(t_\mathrm{p})$ and $\sigma_+ \equiv \sigma(t_+)$, the protocol which yields both maximum efficiency and power reads [24]

$$\lambda_\mathrm{S} = \begin{cases} \frac{T_+}{2\sigma_\mathrm{S}} - \frac{\sqrt{\sigma_+}-\sqrt{\sigma_-}}{\mu t_+\sqrt{\sigma_\mathrm{S}}}, & 0 < t < t_+, \\ \frac{T_-}{2\sigma_\mathrm{S}} + \frac{\sqrt{\sigma_+}-\sqrt{\sigma_-}}{\mu t_-\sqrt{\sigma_\mathrm{S}}}, & t_+ < t < t_\mathrm{p}, \end{cases} \tag{D1}$$

with

$$\sigma_\mathrm{S} = \begin{cases} \frac{\sigma_-}{2}\left[1 + \left(\sqrt{\frac{\sigma_+}{\sigma_-}} - 1\right)\frac{t}{t_+}\right]^2, & 0 < t < t_+, \\ \frac{\sigma_+}{2}\left[1 + \left(\sqrt{\frac{\sigma_-}{\sigma_+}} - 1\right)\frac{t-t_+}{t_-}\right]^2, & t_+ < t < t_\mathrm{p}. \end{cases} \tag{D2}$$

However, this protocol is no longer optimal when one imposes just maximum and minimum values on the response, i.e., $\sigma(t) \in [\sigma_-, \sigma_+]$. Then, our analysis shows that the maximum-efficiency and maximum-power protocol is still of the above form, but with $\sigma_- < \sigma(0) = \sigma(t_\mathrm{p}) < \sigma(t_+) < \sigma_+$.

In Fig. 7, we show the maximum power (a) and maximum efficiency (b) for the trial protocols under the constraint $\sigma_- \equiv \sigma(0) = \sigma(t_\mathrm{p})$ and $\sigma_+ \equiv \sigma(t_+)$. As expected, power and

efficiency corresponding to the protocol λ_S are largest from all the protocols. In particular, the figure demonstrates that the linear protocol, which was found to maximize output power for constrained λ, yields smaller output power than λ_S. And the piecewise constant protocol yields smaller efficiency than λ_S. Nevertheless, it is interesting to note that the performance of the protocol $\lambda_{\text{slow}}(t)$, which optimizes both output power and efficiency for slow driving (see Sec. C for details), is for the chosen parameters indistinguishable from that of λ_S. This means that the chosen cycle is slow enough. Finally, for small enough cycles (small σ_-/σ_+) performances of all the protocols are equal.

[1] G. Pesce, P. H. Jones, O. M. Maragò, and G. Volpe, Optical tweezers: theory and practice, Eur. Phys. J. Plus **135**, 949 (2020).

[2] D. J. Wineland, Nobel lecture: Superposition, entanglement, and raising Schrödinger's cat, Rev. Mod. Phys. **85**, 1103 (2013).

[3] S. Haroche, Nobel lecture: Controlling photons in a box and exploring the quantum to classical boundary, Rev. Mod. Phys. **85**, 1083 (2013).

[4] N. M. Myers, O. Abah, and S. Deffner, Quantum thermodynamic devices: from theoretical proposals to experimental reality, AVS Quantum Sci. **4**, 027101 (2022).

[5] K. Sekimoto, *Stochastic Energetics*, Lecture Notes in Physics Vol. 799 (Springer, Berlin, 2010).

[6] U. Seifert, Stochastic thermodynamics, fluctuation theorems and molecular machines, Rep. Prog. Phys. **75**, 126001 (2012).

[7] F. L. Curzon and B. Ahlborn, Efficiency of a Carnot engine at maximum power output, Am. J. Phys. **43**, 22 (1975).

[8] M. H. Rubin, Optimal configuration of a class of irreversible heat engines. I, Phys. Rev. A **19**, 1272 (1979).

[9] P. Salamon, A. Nitzan, B. Andresen, and R. S. Berry, Minimum entropy production and the optimization of heat engines, Phys. Rev. A **21**, 2115 (1980).

[10] B. Andresen, R. S. Berry, M. J. Ondrechen, and P. Salamon, Thermodynamics for processes in finite time, Acc. Chem. Res. **17**, 266 (1984).

[11] B. Andresen, P. Salamon, and R. S. Berry, Thermodynamics in finite time, Phys. Today **37**(9), 62 (1984).

[12] M. Mozurkewich and R. S. Berry, Finite-time thermodynamics: Engine performance improved by optimized piston motion, Proc. Natl. Acad. Sci. USA **78**, 1986 (1981).

[13] C. Van den Broeck, Thermodynamic Efficiency at Maximum Power, Phys. Rev. Lett. **95**, 190602 (2005).

[14] B. Jiménez de Cisneros and A. C. Hernández, Collective Working Regimes for Coupled Heat Engines, Phys. Rev. Lett. **98**, 130602 (2007).

[15] K. H. Hoffmann, An introduction to endoreversible thermodynamics, AAPP Phys. Math. Nat. Sci. **86**, 1 (2008).

[16] V. Holubec and A. Ryabov, Fluctuations in heat engines, J. Phys. A: Math. Theor. **55**, 013001 (2022).

[17] E. Geva and R. Kosloff, A quantum-mechanical heat engine operating in finite time. a model consisting of spin-1/2 systems as the working fluid, J. Chem. Phys. **96**, 3054 (1992).

[18] A. Parmeggiani, F. Jülicher, A. Ajdari, and J. Prost, Energy transduction of isothermal ratchets: Generic aspects and specific examples close to and far from equilibrium, Phys. Rev. E **60**, 2127 (1999).

[19] T. Hondou and K. Sekimoto, Unattainability of Carnot efficiency in the Brownian heat engine, Phys. Rev. E **62**, 6021 (2000).

[20] T. Feldmann and R. Kosloff, Performance of discrete heat engines and heat pumps in finite time, Phys. Rev. E **61**, 4774 (2000).

[21] R. D. Astumian and P. Hänggi, Brownian motors, Phys. Today **55**(11), 33 (2002).

[22] J. M. R. Parrondo and B. J. de Cisneros, Energetics of brownian motors: a review, Appl. Phys. A **75**, 179 (2002).

[23] P. Reimann, Brownian motors: noisy transport far from equilibrium, Phys. Rep. **361**, 57 (2002).

[24] T. Schmiedl and U. Seifert, Efficiency at maximum power: An analytically solvable model for stochastic heat engines, Europhys. Lett. **81**, 20003 (2008).

[25] Z. C. Tu, Efficiency at maximum power of Feynman's ratchet as a heat engine, J. Phys. A: Math. Theor. **41**, 312003 (2008).

[26] M. Esposito, K. Lindenberg, and C. Van den Broeck, Universality of Efficiency at Maximum Power, Phys. Rev. Lett. **102**, 130602 (2009).

[27] M. Esposito, K. Lindenberg, and C. V. den Broeck, Thermoelectric efficiency at maximum power in a quantum dot, Europhys. Lett. **85**, 60010 (2009).

[28] M. Esposito, R. Kawai, K. Lindenberg, and C. Van den Broeck, Efficiency at Maximum Power of Low-Dissipation Carnot Engines, Phys. Rev. Lett. **105**, 150603 (2010).

[29] O. Abah, J. Roßnagel, G. Jacob, S. Deffner, F. Schmidt-Kaler, K. Singer, and E. Lutz, Single-Ion Heat Engine at Maximum Power, Phys. Rev. Lett. **109**, 203006 (2012).

[30] O. Raz, Y. Subaşı, and R. Pugatch, Geometric Heat Engines Featuring Power that Grows with Efficiency, Phys. Rev. Lett. **116**, 160601 (2016).

[31] V. Holubec and A. Ryabov, Cycling Tames Power Fluctuations near Optimum Efficiency, Phys. Rev. Lett. **121**, 120601 (2018).

[32] K. Brandner and K. Saito, Thermodynamic Geometry of Microscopic Heat Engines, Phys. Rev. Lett. **124**, 040602 (2020).

[33] P. Terrén Alonso, P. Abiuso, M. Perarnau-Llobet, and L. Arrachea, Geometric optimization of nonequilibrium adiabatic thermal machines and implementation in a qubit system, PRX Quantum **3**, 010326 (2022).

[34] V. Cavina, P. A. Erdman, P. Abiuso, L. Tolomeo, and V. Giovannetti, Maximum-power heat engines and refrigerators in the fast-driving regime, Phys. Rev. A **104**, 032226 (2021).

[35] P. A. Erdman, V. Cavina, R. Fazio, F. Taddei, and V. Giovannetti, Maximum power and corresponding efficiency for two-level heat engines and refrigerators: optimality of fast cycles, New J. Phys. **21**, 103049 (2019).

[36] A. Das and V. Mukherjee, Quantum-enhanced finite-time Otto cycle, Phys. Rev. Res. **2**, 033083 (2020).

[37] P. Abiuso and M. Perarnau-Llobet, Optimal Cycles for Low-Dissipation Heat Engines, Phys. Rev. Lett. **124**, 110606 (2020).

[38] T. E. Humphrey, R. Newbury, R. P. Taylor, and H. Linke, Reversible Quantum Brownian Heat Engines for Electrons, Phys. Rev. Lett. **89**, 116801 (2002).

[39] P. Abiuso, H. J. Miller, M. Perarnau-Llobet, and M. Scandi, Geometric optimisation of quantum thermodynamic processes, Entropy **22**, 1076 (2020).

[40] H. J. D. Miller, M. H. Mohammady, M. Perarnau-Llobet, and G. Guarnieri, Thermodynamic Uncertainty Relation in Slowly Driven Quantum Heat Engines, Phys. Rev. Lett. **126**, 210603 (2021).

[41] V. Cavina, A. Mari, and V. Giovannetti, Slow Dynamics and Thermodynamics of Open Quantum Systems, Phys. Rev. Lett. **119**, 050601 (2017).

[42] V. Holubec, An exactly solvable model of a stochastic heat engine: optimization of power, power fluctuations and efficiency, J. Stat. Mech. Theory Exp. **2014**, P05022.

[43] A. Dechant, N. Kiesel, and E. Lutz, Underdamped stochastic heat engine at maximum efficiency, Europhys. Lett. **119**, 50003 (2017).

[44] Y. Zhang, Optimization of stochastic thermodynamic machines, J. Stat. Phys. **178**, 1336 (2020).

[45] P. Abiuso, V. Holubec, J. Anders, Z. Ye, F. Cerisola, and M. Perarnau-Llobet, Thermodynamics and optimal protocols of multidimensional quadratic Brownian systems, J. Phys. Commun. **6**, 063001 (2022).

[46] A. Zhong and M. R. DeWeese, Limited-control optimal protocols arbitrarily far from equilibrium, Phys. Rev. E **106**, 044135 (2022).

[47] M. Bauer, K. Brandner, and U. Seifert, Optimal performance of periodically driven, stochastic heat engines under limited control, Phys. Rev. E **93**, 042112 (2016).

[48] C. A. Plata, D. Guéry-Odelin, E. Trizac, and A. Prados, Optimal work in a harmonic trap with bounded stiffness, Phys. Rev. E **99**, 012140 (2019).

[49] H. Risken, Fokker-planck equation, in *The Fokker-Planck Equation: Methods of Solution and Applications* (Springer, 1996), pp. 63–95.

[50] V. Holubec, A. Ryabov, S. A. M. Loos, and K. Kroy, Equilibrium stochastic delay processes, New J. Phys. **24**, 023021 (2022).

[51] S. Krishnamurthy, S. Ghosh, D. Chatterji, R. Ganapathy, and A. K. Sood, A micrometre-sized heat engine operating between bacterial reservoirs, Nat. Phys. **12**, 1134 (2016).

[52] V. Holubec, S. Steffenoni, G. Falasco, and K. Kroy, Active Brownian heat engines, Phys. Rev. Res. **2**, 043262 (2020).

[53] A. Kumari, P. S. Pal, A. Saha, and S. Lahiri, Stochastic heat engine using an active particle, Phys. Rev. E **101**, 032109 (2020).

[54] G. Gronchi and A. Puglisi, Optimization of an active heat engine, Phys. Rev. E **103**, 052134 (2021).

[55] I. A. Martínez, E. Roldán, L. Dinis, D. Petrov, and R. A. Rica, Adiabatic Processes Realized with a Trapped Brownian Particle, Phys. Rev. Lett. **114**, 120601 (2015).

[56] D. Arold, A. Dechant, and E. Lutz, Heat leakage in overdamped harmonic systems, Phys. Rev. E **97**, 022131 (2018).

[57] V. Blickle and C. Bechinger, Realization of a micrometre-sized stochastic heat engine, Nat. Phys. **8**, 143 (2012).

[58] V. Holubec and A. Ryabov, Diverging, but negligible power at carnot efficiency: Theory and experiment, Phys. Rev. E **96**, 062107 (2017).

[59] V. Cavina, A. Mari, A. Carlini, and V. Giovannetti, Optimal thermodynamic control in open quantum systems, Phys. Rev. A **98**, 012139 (2018).

[60] I. A. Martínez, É. Roldán, L. Dinis, D. Petrov, J. M. R. Parrondo, and R. A. Rica, Brownian carnot engine, Nat. Phys. **12**, 67 (2016).

[61] I. A. Martínez, É. Roldán, L. Dinis, and R. A. Rica, Colloidal heat engines: a review, Soft Matter **13**, 22 (2017).

[62] T. Schmiedl and U. Seifert, Optimal Finite-Time Processes In Stochastic Thermodynamics, Phys. Rev. Lett. **98**, 108301 (2007).

[63] H. Then and A. Engel, Computing the optimal protocol for finite-time processes in stochastic thermodynamics, Phys. Rev. E **77**, 041105 (2008).

[64] V. Holubec and A. Ryabov, Efficiency at and near maximum power of low-dissipation heat engines, Phys. Rev. E **92**, 052125 (2015).

[65] T. R. Gingrich, G. M. Rotskoff, G. E. Crooks, and P. L. Geissler, Near-optimal protocols in complex nonequilibrium transformations, Proc. Natl. Acad. Sci. USA **113**, 10263 (2016).

[66] P. A. Erdman and F. Noé, Identifying optimal cycles in quantum thermal machines with reinforcement-learning, NPJ Quantum Inf. **8**, 1 (2022).

[67] I. Khait, J. Carrasquilla, and D. Segal, Optimal control of quantum thermal machines using machine learning, Phys. Rev. Res. **4**, L012029 (2022).

[68] A. Dechant and Y. Sakurai, Thermodynamic interpretation of Wasserstein distance, arXiv:1912.08405.

[69] T. Van Vu and Y. Hasegawa, Geometrical Bounds of the Irreversibility in Markovian Systems, Phys. Rev. Lett. **126**, 010601 (2021).

[70] M. Carrega, L. M. Cangemi, G. De Filippis, V. Cataudella, G. Benenti, and M. Sassetti, Engineering dynamical couplings for quantum thermodynamic tasks, PRX Quantum **3**, 010323 (2022).

[71] N. Pancotti, M. Scandi, M. T. Mitchison, and M. Perarnau-Llobet, Speed-Ups to Isothermality: Enhanced Quantum Thermal Machines through Control of the System-Bath Coupling, Phys. Rev. X **10**, 031015 (2020).

[72] V. Holubec, *Non-equilibrium Energy Transformation Processes: Theoretical Description at the Level of Molecular Structures*, Springer Theses (Springer International, Cham, 2014).

[73] V. Holubec and A. Ryabov, Maximum efficiency of low-dissipation heat engines at arbitrary power, J. Stat. Mech. Theory Exp. (2016) 073204.